

RollingLight: Universal Camera Communications for Single LED

Hui-Yu Lee, and Hsin-Mu Tsai
Department of Computer Science and Information Engineering
National Taiwan University
Taipei, Taiwan
{r01922028, hsinmu} @csie.ntu.edu.tw

ABSTRACT

The paper presents RollingLight, a visible light communication (VLC) system that utilizes a single LED light source as the transmitter and a CMOS rolling shutter camera as the receiver. In our system, we propose the use of Rolling Shutter Frequency Shift Keying (RS-FSK), a very simple modulation that can be implemented with very low cost embedded microprocessors, thus enabling LEDs that already exist in our daily life, such as LED indicators in electronics and light fixtures, to “talk”. Today, almost every modern mobile device is equipped with at least one built-in CMOS rolling shutter camera, and it can receive signals from the LEDs without any modification, and thus, any additional cost. Our idea is to use the acquired images from the rolling shutter camera to extract the message transmitted from the LED. This technology can be used in many applications, such as advanced driver assistance system (ADAS), indoor positioning, advertising, and problem diagnosis. Our system allows rolling shutter cameras with different hardware specifications such as resolution, frame rate, read-out time, and exposure time, to all have the capability to decode the transmission, and the decoding performance scales with the camera specifications. In addition, the transmission is not visible to human eyes, thus keeping the original illumination or signaling function of the LEDs. Our design is evaluated with experiments performed with a range of different cameras. The RS-FSK modulation scheme can be used to transmit data at 11.25 bytes per second. We also develop a real-time application on the smartphone.

Categories and Subject Descriptors

C.2.1 [Network Architecture and Design]: Wireless Communication; B.4.1 [Data Communications Devices]; C.3 [Special-Purpose and Application-Based Systems]

Keywords

Visible Light Communications, Camera Communication, Rolling Shutter, Frequency Shift Keying, smartphones

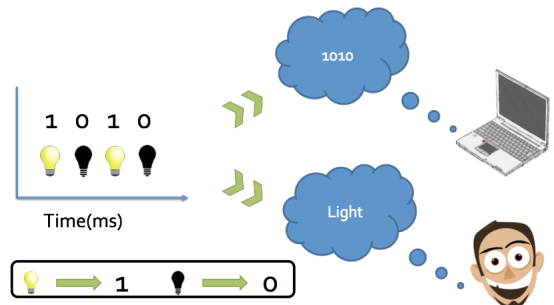


Figure 1: A schematic diagram of VLC

1. INTRODUCTION

Visible light communications (VLC) have gained wide attention in the research community recently. The possibilities of using every light emitting diode (LED) that already exists in our daily life to talk and to serve as a new pervasive communication infrastructure are endless - it enables interference-free, secure, low cost, and energy efficient short range communications to a wide range of electronic devices and appliances, from cars with LED taillights, light fixtures with LED light bulbs, to refrigerators with tiny LED indicators. Figure 1 illustrates how VLC works. VLC uses the optical signal to carry digital information by controlling the LED's light intensity in free space. When the light is transmitting, due to persistence of vision, human eyes cannot perceive the transmissions.

This work implements a form of VLC that uses a **single LED** as the transmitter and a Complementary Metal-Oxide-Semiconductor (CMOS) **rolling shutter camera sensor** as the receiver, a form of Camera Communications (CamCom). We chose to develop this form of VLC due to the universal availability of both the transmitting component - a simple LED (as opposed to an array of LEDs or an LCD screen), and the receiving component - a CMOS camera. Almost every modern mobile device, including smartphones, tablets, and laptops, is equipped with at least one built-in CMOS camera. We believe that this would be the best paradigm

to jump-start the VLC technology in the market. As a result, one of the most important objectives of our work is to ensure the compatibility of a wide range of unmodified CMOS cameras to the LEDs transmission.

One very important advantage of CamCom is that the acquired images during the receiving process provide a means to **visually associate** the transmitting object with the transmissions, since the receiver has the knowledge of which pixels in the images are transmitting. We can use the idea in many applications. One is **Advanced Driver Assistance System (ADAS)**. we can use the LED tail lights of the front car to transmit a message to the camera of the rear cars. The message can contain safety-related status information, such as speed, location, heading, and brake/turn signal status, or user-specified short text messages to form an advanced driver assistance system.

Another example is **indoor positioning**. We receive the light ID transmitted by the LED light and obtain the vertical distance between the receiver and the transmitting lights, and the horizontal distances between the lights. Then, we can calculate the relative position and know where we are in the building.

We also can use the LED lights for **advertising**. For example, in a supermarket, we can use the LED light on the shelf to transmit the sale and discount information of the goods. We can use the traffic lights and signs to tell us the road status ahead.

Besides, we can apply this kind of communication for **system diagnosis**. For example, when a scooter breaks down, we can transmit the sensor log via the LED tail lights to briefly check and detect the problem of the scooter; in a server room, full of machines on the racks, it is often hard to find out which server is having trouble, the nature of the problem, and the IP address of the machine. Imagine if each server has VLC capability on one of its high brightness LED, then we can point our smartphone's camera at an array of servers, and immediately these information will be shown right next to the server, for the administrator to diagnose the problem in an easier way.

In this work, we presented a **theoretical model** to describe the single-LED-to-rolling-shutter-camera channel. Furthermore, we proposed the **Rolling Shutter-Frequency Shift Keying (RS-FSK)** modulation and demonstrated that the modulation is compatible to a wide range of CMOS cameras with different resolution, read-out time, and exposure time, satisfies the lighting requirements, and can be implemented with cost-efficient hardware.

However, as the transmitting light and the receiving camera are not synchronized, the transmitting frame rate and the receiving frame rate are not usually the same. When the transmitting frame rate is higher than the receiving frame rate, there could be symbol loss.

When the transmitting frame rate is lower than the receiving frame rate, reception of redundant symbols is possible. Although no information is lost, the receiver still needs to detect the redundant symbol so that it can be dropped to obtained the correct symbol sequence.

A more common event when the transmitting frame duration and the receiving frame duration are different is that there could be multiple image areas each corresponding to a symbol. In other word, a mix of different symbols in a single received image frame. A mixed frame is a very common and periodic event. Even when the transmitting and the receiving frame durations are very close to each other, mixed frames would be received because of the phase difference between transmitter and receiver.

Therefore, in this paper we present a scheme that can handle **unsynchronized** transmitter and receiver pairs. We also implement the entire system and evaluate whether packet reception rate can be improved.

2. BACKGROUND AND RELATED WORK

2.1 Camera-received VLC

2.1.1 Screen-to-camera communications

A number of prior works [1, 2, 3] utilized cameras as the receiver to implement one-way communication links. Those works utilized a LCD screen as the transmitter. The main benefit of this approach is that both the ability to display different colors and the high resolution of the LCD could be fully exploited, to improve the data rate.

PixNet [1] utilized the large quantity of pixels on a LCD to form OFDM symbols to transmit data to the camera receiver, and the implemented prototype has perspective correction ability.

COBRA [2] proposed a similar approach that uses pixels as as barcodes and utilized the color information of pixels to achieve higher signal to noise ratio. These works, however, did not solve the problems raised by the unsynchronized transmitter and receiver pair. The presented solution is to repeat the same packet transmission twice in order to guarantee the reception of all signal segments.

LightSync [3] introduces inter-frame erasure coding and line sequence number to reduce the high packet error rate due to synchronization issues. The approach also actively filters out rolling-shutter effects.

VRCodes (NewsFlash) [4] takes advantage of the rolling shutter effect to decode visual tags displayed on LCDs. The tags use multiple pixels of different colors, modulated at up to 120Hz to transmit data. The technology exploits the "flicker-fusion threshold" of the human eye to blend the tags into the background by rapidly flashing complimentary hues of color, still visible to a

rolling shutter camera. This work suggests how different color channels could be used to increase data throughput, while still keeping transmissions imperceptible to humans.

Visual MIMO [5, 6, 7] is a method that uses any light-emitting spatial array as the transmitter and uses ordinary cameras as the receivers. It proposes a photometric modeling for hidden imagery and can realize a dual use of the electronic display: to display an image for human observation while simultaneously transmitting hidden bits for decoding by a camera.

Compared to these works, we proposed to use only a single LED light as the transmitter and a commonly available CMOS camera as the receiver, and many design considerations are not the same as these prior research works utilizing multiple optical transmitting sources.

2.1.2 Single-LED-to-camera communications

Three works [8, 9, 10] have previously investigated how to implement single-LED-to-camera communication links. In [8], the author proposes undersampled frequency shift OOK (UFSOOK), which allows the use of a high signal frequency while the modulation can still be decoded by a common camera with 30 fps (frame rate per second). The scheme is compatible to both global shutter and rolling shutter cameras, but the maximum achievable data rate is only half of the frame rate per light source.

In [9], the authors utilized rolling shutter sampling to encode data with Manchester coding at high symbol rate, and was the first work to take advantage of the rolling shutter to implement CamCom. However, the implementation exhibits a high packet drop rate due to the long processing time of the decoder application per frame and lack of considerations for synchronization issues. Thus, the reception is not continuous and some frames are inevitably lost. The transmitter then needs to send signal. In addition, the transmitting light needs to illuminate the entire image for the receiver to demodulate the transmission. We can achieve a data rate much higher than 50% of the frame rate per light source, and have designs to address the issues caused by the exposure operation of the camera and unsynchronized nature of the communication link. A further drawback in this work is that the modulated signal can produce a human perceivable flicker from transmitting LED. The authors alleviate this by imposing a DC bias on the signal, which in turn decreases its dynamic range and SNR at the receiver. This makes the scheme require significantly brighter lights and more complex driving hardware than our proposed approach.

In [10], the author used binary frequency shift keying (BFSK) of a high frequency PWM signal to encode data that can be used as localization landmarks. On the receiver side, they exploited rolling shutter camera sen-

sors to detect high-frequency changes in the intensity of light reflected off surfaces, which is indirect line-of-sight of the camera. The data rate is only 1.25 bytes per second (the authors claimed that it is fast enough to send an ID code) while in our work there is a need to increase the data rate to communicate rather than just perform localization. To detect the transmitting frequency, they used 1-D fast Fourier transform. However, we have tried the FFT method before and it usually requires a threshold to eliminate the noise. It is hard to have a general threshold which can be adopted in different environments. For the receiver which is unsynchronized with the transmitter, they proposed a sliding window approach where they first stitch all of the captured frames together into a single, long image. Then they can detect the frequency by sliding the window and locating the window position corresponding to the highest power. However, we can stitch the images only if the light is full of whole image (for example, reflected from the surface). Moreover, if there is a symbol loss between the two frames, then the result of stitching images would likely be inaccurate. In our work, we use additional schemes to address these problems.

2.2 Channel Model of Rolling Shutter Camera

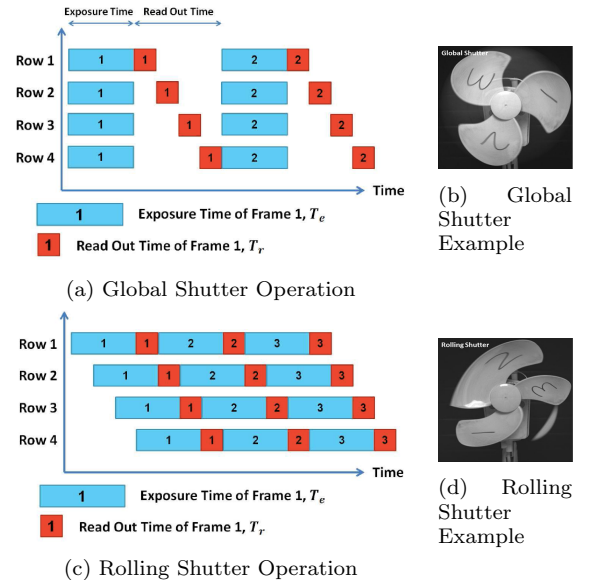
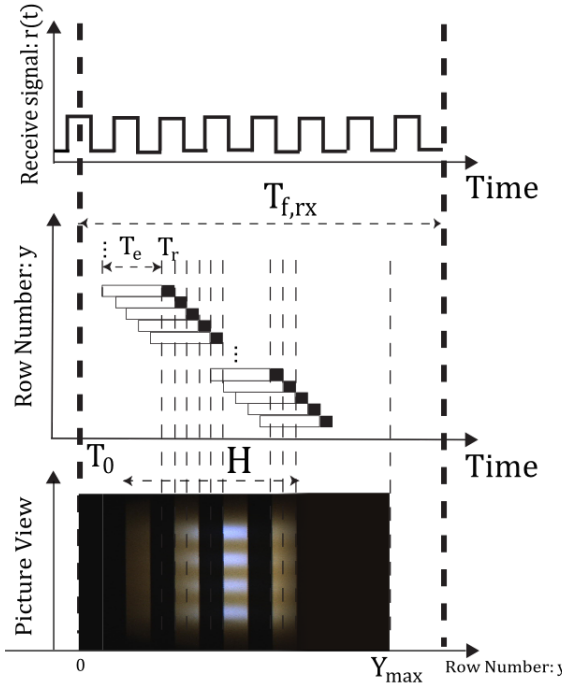


Figure 2: Shutter mechanisms

2.2.1 Rolling Shutter Operation

Figure 2 compares global and rolling shutter operation [11]. Global shutters, which are commonly implemented on CCD sensors, expose all pixels on the sensor simultaneously and gather incoming light over all pixels during the exposure time. Although some CMOS sensors use a global shutter, the majority found in the

consumer market utilize a rolling shutter. One of the key properties of a rolling shutter camera sensor is its sequential read-out architecture. As in most CMOS sensors there is no per pixel storage to hold the accumulated charge during the exposure operation, the exposure period happens right before each read-out operation. The read-out architecture can process charge voltage signals one row at a time. Since the read-out durations of two rows cannot overlap, each of the exposure durations of a row of pixels is shifted by a fixed amount of read-out time (represented by T_r in [Figure 3](#)), resulting in the so-called rolling shutter operation. For each pixel, the incoming intensity modulated signal is integrated for a time period called exposure time (represented by T_e in [Figure 3](#)).



[Figure 3](#): The receiving operation of a rolling shutter camera sensor. Top: the original received signal; middle: the exposure and read-out processes; bottom: the resulted image. $T_{f,rx}$: receiving frame duration; T_e : exposure time; T_r : read-out time.

[Figure 3](#) shows the receiving operation of a rolling shutter camera sensor to an intensity modulated signal. Assume the original received signal in time is given by $r(t)$, which includes the signal from the transmitted light and other ambient interference. Considering the direct integration operation taking place during exposure and the rolling shutter operation, the intensity of a pixel in y -th row in the image, $I[y]$, which also represents the total amount of photons received by the pixel during exposure, is given by:

$$I[y] = \int_{T_0+yT_r}^{T_0+yT_r+T_e} r(t)dt, 0 \leq y \leq Y_{\max}, \quad (1)$$

where T_r is the read-out time, T_e is the exposure time, T_0 is a reference time point that corresponds to the start of the exposure time of the first row of pixels in the image, and Y_{\max} is the number of rows of pixels in the image. Note that the transmitting light might not illuminate all rows in the image. In that case, the transmitted signal is only observed in $I[Y_{\text{top}} \leq y \leq Y_{\text{top}} + H]$, where H represents the height of the image area illuminated by the transmitting light.

The direct integration operation can be considered as a low-pass filter (or a moving average filter), and thus $I[y], 0 \leq y \leq Y_{\max}$ is a filtered version of the original received signal $r(t)$. The filter distorts high frequency components in the received signal, especially the ones with a frequency higher than $1/T_e$.

2.2.2 Time Gap in the Frame Duration

Utilizing [Equation 1](#), if the transmitting light occupies all rows of pixels in the image, the end of exposure of the last row in this image frame is $T_0 + Y_{\max}T_r + T_e$, while the start of exposure of the first row in the next image frame is $T_0 + T_{f,rx}$. The **time gap** between these two events $T_{f,rx} - Y_{\max}T_r - T_e$, when T_e is small, is significant for most cameras. This is the amount of time during which the camera is not performing any exposure operation, i.e., not receiving the transmitted signal. Signal transmitted during this time period is lost. [Table 1](#) summarizes both the values of this time gap (without subtracting the exposure time T_e) and the percentage of time contributed by this time gap compared to a frame duration. Note that for some cameras, this could be up to half of the receiving frame duration. In addition, in the case that the transmitting light does not illuminate all rows in the image, this time gap could further increase.

2.2.3 Channel Characteristics

In summary, the single-LED-to-rolling-shutter-camera channel exhibits two major characteristics:

1. The signal that can be obtained from the image is a low-pass filtered version of the original received signal in time. The filter creates distortions in high frequency components.
2. The receiving process is not continuous. This can be considered as a form of channel fading; when it takes place, the channel loss is infinite. The ratio of signal lost is determined by a constant time gap that depends on camera parameters, and the size of the image area illuminated by the transmitting light. A smaller image area corresponds to a higher ratio of signal lost.

Table 1: Summary of Camera Parameters

	Image Resolution ($X_{\max} \times Y_{\max}$)	Frame Rate (fps)	Measured Read-out Time (μs)	Time Gap (ms) (Percentage of Frame Duration)
Point Grey Flea3	2048x1080	30	14.75	17.40 (52.23%)
Apple iPhone 5S	1920x1080	29.98	19.15	12.67 (37.99%)
Apple iPhone 4S	1920x1080	29.87	24.48	7.04 (21.03%)
HTC New One	1920x1080	30	18.79	13.04 (39.11%)
Apple iPhone 4	1280x720	29.97	44.88	1.05 (3.15%)
HTC Desire HD	800x480	29.08	55.18	7.90 (22.97%)
Google Nexus One	720x480	30.57	59.66	4.07 (12.45%)

3. CHALLENGES & SYSTEM OVERVIEW

test intro

4. ROLLINGLIGHT DESIGN

4.1 Rolling Shutter Frequency-Shift Keying (RS-FSK)

4.1.1 Modulation

The fundamental idea of RS-FSK is to use the square waves of a number of different **frequencies** as different symbols, mapped to different bit patterns of the same length. The signal of the i -th symbol is represented by the fundamental frequency f_i of the square wave:

$$s_i(t) = I_{\max} \left[\frac{\cos(2\pi f_i t)}{2} \right] \quad (2)$$

where I_{\max} is the maximum output intensity of the transmitting light.

A frequency modulation is advantageous in the following aspects: (1) The transmitted frequency can be demodulated by receivers with different sampling rate, as long as the sampling rate satisfies the Nyquist rate requirement. This implies that cameras with different read-out time are all compatible to a single transmission signal format. (2) Demodulation is still possible when some segments of signal samples are lost in a symbol period, as long as the longest remaining signal segment has a length larger than the transmitted signal period. This addresses the time gap challenge previously described. (3) The average intensity stays the same for all symbols, implying that the transmission is not observable by human eyes as long as the frequency is higher than 100 Hz.

In addition, a square wave has some key properties which make it suitable for our purposes: (1) It survives the moving average filtering mechanism due to the exposure operation, as long as the signal period is not an integer multiple of the exposure time. This is true even for very long exposure time. Most important of all, the fundamental frequency of the square wave remains

the same and accurately observable after filtering. (2) It is extremely simple and can be implemented with cheap microcontrollers or PWM driver chips. No DAC is needed to output signal at different amplitude levels. (3) The modulation supports dimming by transmitting a modified square wave at the same frequency, but with different ratio of ON state and OFF state, i.e., duty cycle.

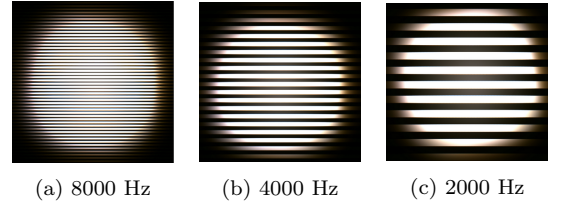


Figure 4: Received images of different transmitting frequencies.

Figure 4 shows the received images of different transmitting frequencies.

4.1.2 Demodulation

The transmitted signal period is the inverse of the transmitted signal frequency f_i . To obtain the **signal period**, we need to know the pixel width of strip in the received image first. In Figure 5, as rows of pixels are sequentially obtained with sampling period T_r , one cycle of square wave transmission results in a pair of bright strip and dark strip in the image. The sum of whole widths is given by

$$W = \frac{1}{f_i T_r} \quad . \quad (3)$$

Note that the width of the bright strip could be larger than the width of the dark strip in the image. This is due to blooming, the overflow of charge from a saturated pixel into its neighboring pixel [12]. We thus consider the widths of the bright strip and the dark strip together in the calculation, to average out the effect. Since W might not be an integer, averaging the observed widths over a large image area would help to improve the accu-

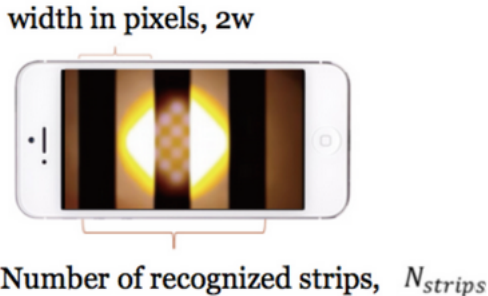


Figure 5: Received strips: w pixel

racy of the estimate of the width. Then, the transmitted period $1/f_i$ can be calculated with [Equation 3](#).

To have a more robust method to accurately determine the period of the signal, i.e., the average width of a pair of bright and dark strips in the image, we modified a well-known pitch detection algorithm (PDA), YIN [\[13\]](#), that is originally designed to determine the fundamental frequency of a segment of audio signal in speech or music. We chose to use a method that operates in time domain, so that computationally expensive Fourier Transform operation can be avoided.

We start by summing up all pixels in each row

$$I[y] = \sum_{x=1}^{X_{\max}} I[x][y] , \quad (4)$$

obtaining a one-dimensional signal, where $I[x][y]$ is the intensity (luminance)¹ of the pixel at location (x, y) in the received image. This operation uses pixels in different columns for redundancy, averaging out noises that exists in different columns of pixel.

To find the period of the periodic signal presented in $I[y]$, a difference function may be constructed:

$$d_{\Delta}(\delta) = \sum_{y=1}^{H/2-1} (I[y] - I[y + \delta])^2 \quad (5)$$

and we search for the values of δ that are closest to zero. Note that δ represents both the shift in space in number of pixels and the shift in time in multiples of read-out time of the camera. As pointed out in [\[13\]](#), using the difference function instead of the standard autocorrelation function (ACF) can avoid a large portion of the error caused by change of amplitudes in the signal, causing by the change of luminance in different rows of pixels. An added advantage is that subtraction is computationally more efficient than multiplication.

Another possible source of error happens at small δ values, since when $\delta < \frac{1}{fT_r}$, the difference function

could produce a large value due to the fact that we use square waves - there is no significant change of signal amplitude except at the sharp transitions. We instead use cumulative mean normalized difference function (CMNDF) [\[13\]](#) to mitigate this problem:

$$d'_{\Delta}(\delta) = \begin{cases} 1, & \text{if } \delta = \{0, 1\} \\ d_{\Delta}(\delta) / \left[(1/\delta) \sum_{j=1}^{\delta} d_{\Delta}(j) \right] & \text{otherwise.} \end{cases} \quad (6)$$

The function now starts from 1 at $\delta = 0$ and remains large with small δ values, and only drops below 1 when $d'_{\Delta}(\delta)$ falls below average. The smallest local minimum in $d'_{\Delta}(0 \leq \delta \leq H/2 - 1)$ is then located and serves as the period estimate of the received signal.

Using CMNDF, the system can determine the period of the transmitted signal with a resolution of read-out time. However, as the period of the signal is not always an integer multiple of the read-out time, i.e., the sampling period, the output could results in error up to half of the read-out time. We again resort to the method proposed in [\[13\]](#) - to use parabolic interpolation to estimate the location of the actual minimum that could exist between samples. Assuming that $\hat{\delta}$ is the integer value that corresponds to the smallest minimum in $d'_{\Delta}(\delta)$, this method only needs three function values, $y_{-1} = d'_{\Delta}(\hat{\delta} - 1)$, $y_0 = d'_{\Delta}(\hat{\delta})$, and $y_{+1} = d'_{\Delta}(\hat{\delta} + 1)$, to determine the new estimate:

$$\hat{\delta}' = \hat{\delta} + \frac{y_{+1} - y_{-1}}{2(2y_0 - y_{+1} - y_{-1})} \quad (7)$$

With parabolic interpolation, our modified YIN algorithm can very accurately determine the period of the transmitted signal. Note that the output of the algorithm is in pixel. It can be converted back to be in unit of time by multiplying the number with T_r .

4.2 Problem Statement: Unsynchronized Transmitter and Receiver

4.2.1 The Problem

As the transmitting light and the receiving camera are not synchronized, the transmitting frame rate and the receiving frame rate are usually not the same. As mentioned in [\[3\]](#), the received frame rate exhibits more variability for several reasons. For example, HTC One X camera appears to record videos are 24 fps, but the camera callback API can only support saving the frames at 15 to 20 fps. The callback slows down when there is insufficient memory available in the system. The frame rate on the Samsung Galaxy S III is only stable if the CPU is locked to its maximum frequency with its setCPU app. Otherwise, it fluctuates hugely between 21 to 29 fps for an entirely white foreground, and have an average of around 25 fps. Even when the frame rate appears steady, the inter-frame interval still varies. In our design, we assume that the ratio $f_{ps_{tx}} / f_{ps_{rx}}$

¹If the obtained image is in RGB instead of grayscale, it needs to be converted to obtain the luminance information.

is not more than 2 or less than 0.9, which means the receive frame rate is between 15 and 33 fps when the transmitting frame rate is 30 fps. Note that this can be changed with straightforward modifications to our design to allow a larger variability of frame rate.

Received frame patterns. Given various potential combinations of the transmitting and receiving frame rates, we perform a simple experiment to study the received frame pattern. We transmit the data at several frame rates, and record the video with the PointGrey Flea3 camera [14] with 30 fps.

Figure 6 shows the received frame pattern. For each received frame, we can detect which of the originally transmitted frames corresponds to it, and plot a circle for each detected frame.

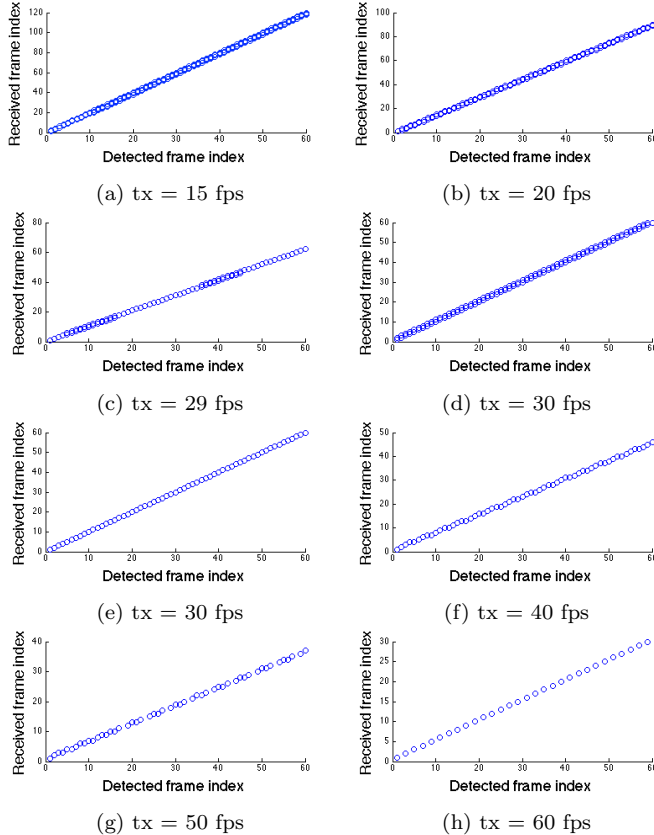


Figure 6: Received frame patterns under different tx fps

When two or more detected frame indices correspond to the same received frame index, this captured frame contains a **mixture of two or more transmitted symbols**. When two or more received frame indices correspond to the same detected frame index, these captured frames have **redundant transmitted symbols**. Any gap between consecutive received frame indices indicates a **symbol loss**.

At 15 fps and 20 fps, we capture at least one complete frame with a full symbol. However, other frames show that the mixed frames and redundant frames are also

possible due to random phase offsets.

When the transmitting rate is close to the receiving rate - 30 fps, mixed frames would be received for a few consecutive frames. Even when the transmitting frame rate is exactly 30 fps, mixed frames can still occur, in which case, it would always be the case received due to the constant phase offset, as shown in Figure 6(d). In the other case, a single transmitted symbol would always be received in each frame, as shown in Figure 6(e).

As the transmitting rate increases further, we start to experience mixed and missed symbols at times.

Since the camera records the videos at 30 fps, detecting the same number of transmitted frames requires receiving far more frames at a low transmitting rate. Therefore, the scales of the vertical axis are different across the subfigures of Figure 6.

4.2.2 The Probability

To figure out the symbol loss and mixed frame problems, we first want to know how often do they happen, thus we derive the probabilities under different conditions. In addition, we want to know what factors affect them and how to address them.

Case I: When the transmitting frame rate is higher than the receiving frame rate, there could be symbol loss, defined as no part of the transmitting frame duration of a particular symbol is covered by the exposure time of any receiving image frame. Figure 7 illustrates the missing symbols. Let the transmitting frame duration be $T_{f,tx}$ (symbol time), the receiving frame duration be $T_{f,rx}$, and the Y size of the image area illuminated by the transmitting light be H . The gray part is the time gap that the camera is not receiving the transmitting symbols. If $T_{f,tx} < T_{f,rx} - HT_r$, which means the transmitting symbols may appear in the gray part, then a symbol loss is possible. In that case, the probability of a symbol lost is given by

$$P_{\text{miss}} = \frac{T_{f,rx} - HT_r - T_{f,tx}}{T_{f,rx}} . \quad (8)$$

We can see that the probability of the symbol loss in Figure 7 is around 1/2, which means there is a symbol loss followed by every received symbol.

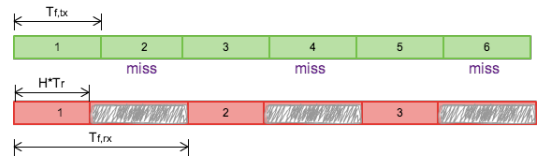


Figure 7: Missing symbol illustration.

A more common event which could happen when the transmitting frame duration and the receiving frame duration are different is that in a single image frame there could be multiple image areas each corresponding to

a symbol. In other words, a mix of different symbols in a single receiving image frame. [Figure 8](#) illustrates the mixed frames. If the boundary between two consecutive transmitting symbols locates in the red part, during which the camera is receiving the transmitting symbols, then there is a mixed frame. The probability for this event is given by

$$P_{\text{mix}} = \begin{cases} \frac{HT_r}{T_{f,tx}}, & \text{if } T_{f,tx} \geq HT_r \\ 1, & \text{otherwise.} \end{cases} \quad (9)$$

We can see that the probability of the mixed frame in [Figure 8](#) is around 1/3.

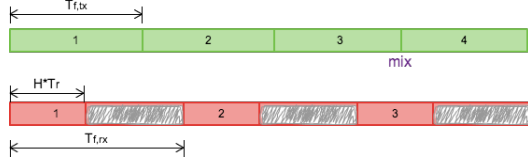


[Figure 8](#): Mixed frame illustration.

A mixed frame is a very common and periodic event. Even when the transmitting and the receiving frame durations are very close to each other, mixed frames would be received for a few consecutive frames. After receiving a few frames with only a single symbol, consecutive mixed frame would appear again. [Figure 9](#) shows the received frame with mixed symbols. If the boundary of the image areas corresponding to different symbols is not determined, then the period detection algorithm would output one value. The value would usually be closer to the signal period of the symbol that occupies a larger image area, but usually has a large error.

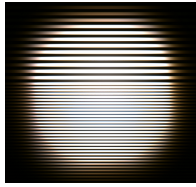


[Figure 9](#): Received frame with mixed symbols.

Case II: When the transmitting frame rate is lower than the receiving frame rate, a redundant symbol is possible. Although no information is lost, the receiver still needs to detect a redundant symbol so that it can be dropped to obtain the correct symbol sequence.

On the other hand, a mixed frame is also possible in this case. The probability for a mixed frame is given by

$$P_{\text{mix}} = \frac{HT_r}{T_{f,tx}} \quad . \quad (10)$$

which is same as the probability in Case I. We can see that the probability of the mixed frame in [Figure 10](#) is around 1/3.

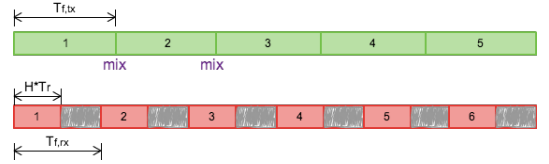


[Figure 10](#): Mixed frame illustration.

According to the probability of lost symbol and mixed frame, the transmitting frame duration ($T_{f,tx}$), the receiving frame duration ($T_{f,rx}$), the height of the LED in the image (H), and the read-out time of camera sensor (T_r) and the factors which may affect the probabilities. We will introduce and evaluate how well our design address these issues in the following chapters.

4.3 System Architecture and End-to-End System Flow

This section describes the overall end-to-end system flow.

Bit-to-symbol mapping. Data bits to be transmitted will first be split into bit patterns of a constant length. Each bit pattern is then mapped to a data symbol.

Parity symbol. As symbols could be lost or corrupted due to the time gap of the channel or if the exposure time is an integer multiple of the signal period, a parity symbol is inserted for every n data symbols by **XOR-ing** all n data symbols, so that if only one of the n data symbols or the parity symbol is not correctly received, the receiver can **recover the lost symbol**. The number of parity symbols that should be added to a packet can be determined by calculating expected number of lost symbols in a packet using the probability equation in [subsubsection 4.2.2](#).

Sequence number. After constructing a sequence of symbols, including the parity symbol, to be transmitted, we label each symbol with a **1.5 bit** sequence number $= \{0, 1, 2\}$. The sequence number can be obtained by calculating the index number modulo 3. The sequence number is then combined with the data symbol to become one meta symbol, then mapped to one of the selected signal periods. Note that the sequence number reduces the number of bits that can be represented by each symbol by 1.5 bits. However, this is required to detect **lost symbols** (when the transmitting frame duration is smaller than the receiving frame duration) or **redundant symbols** (when the transmitting frame duration is larger than the receiving frame duration). Taking the assumption into consideration, it can be proved that there could be no consecutive symbol losses. Thus, a 1.5 bit sequence number, $\{0, 1, 2\}$, would be sufficient determine the location of a lost symbol in the sequence. Note that the sequence number will be represented by the most significant 1.5 bits in a sym-

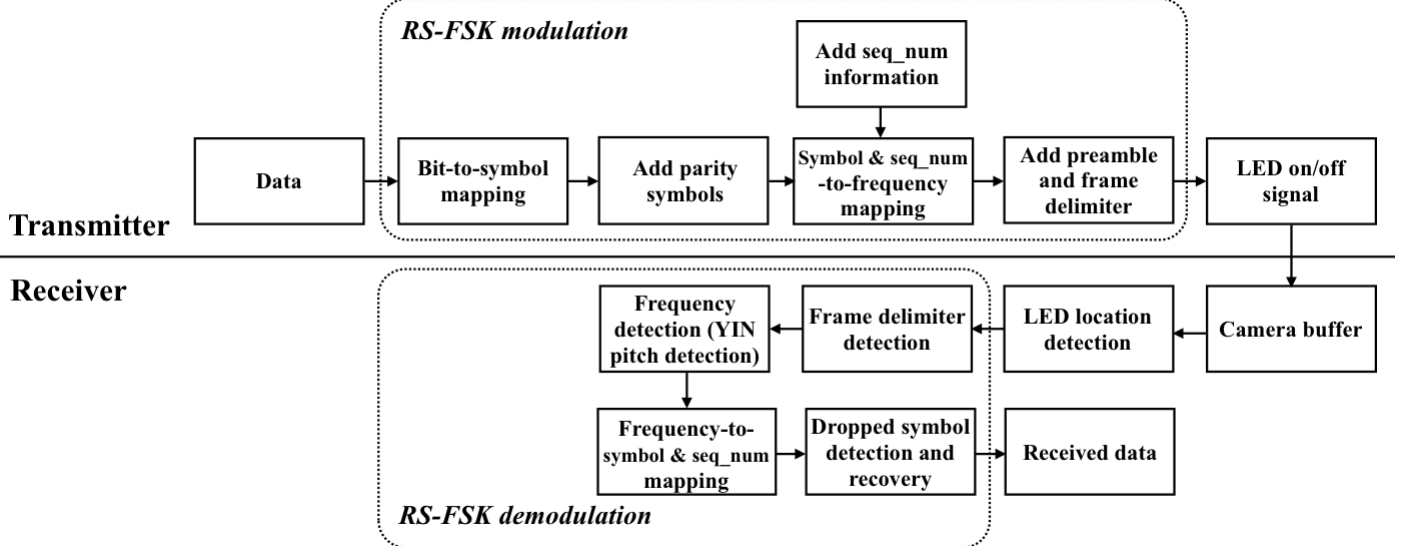


Figure 11: Block Diagram of our Proposed System

bol, i.e., symbols with different sequence numbers will be separated with a large margin, and thus getting an erroneous sequence number is unlikely.

Preamble symbol. Next, the preamble symbol, which has a signal period known to the receiver, is inserted at the beginning of the symbol sequence. The preamble symbol serves two functions: one is for the receiver to detect the start of the packet and start the subsequent demodulation process, while the other is for the receiver to accurately **calibrate its T_r value** based on the period estimate of the preamble, so that the error of the period estimates of all subsequent symbols in this packet can be minimized. As a result, the signal period with the smallest error variation is selected as the period for the preamble symbol. In our experiment, we select the 5657.3886 Hz as the period for the preamble symbol. This is the highest frequency used in our design.

Symbol delimiter. Finally, another signal period is selected as the symbol delimiter signal period. In order to easily **separate consecutive symbols** in the same image, i.e., two areas in the image showing signals with different periods, a signal with this signal period will be transmitted for a short duration between any two symbol transmissions. The transmitting light is then driven to transmit a sequence of square waves according to pre-determined list of signal periods representing the entire data packet.

Figure 12 shows an example flow of the transmitter end. The message "hello!" is converted to the bit string, Then every 4-bit is mapped to a symbol. Assume the P_{miss} is 0.25, which means a parity symbol is inserted for every 3 symbols. Next step we tag the symbols (in-

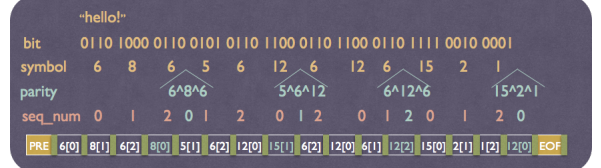


Figure 12: An example flow of the transmitter end.

cluding parity symbol) in the order of $\{0, 1, 2\}$ as the sequence number. The last step is to add the preamble symbol and the EOF symbol (the yellow part in the figure) at the beginning and the end of the data, and the symbol delimiter symbol (the green part in the figure) between each data symbols.

LED location detection. The receiving camera captures a series of images with the transmitting light. The receiver starts the demodulation process by determining the image area occupied by the transmitting light. In our system, this is done by extracting an area with very high intensity values. More sophisticated detection and tracking algorithms based on computer vision techniques can be utilized if necessary.

Symbol delimiter detection. A symbol delimiter detector is then executed to determine whether a symbol delimiter area presents in the image. Figure 13 shows the received image which contains a symbol delimiter. The detection step is done by calculating the value of the difference function described in subsubsection 4.1.2 for all possible symbol delimiter locations in the image, but only with a fixed shift value that equals the the signal period of the symbol delimiter. If the minimum value of the function for all possible delimiter locations is larger than a pre-defined threshold, then it

will output the location of the symbol delimiter. Then, the period detection algorithm can be executed to determine the signal periods of two image areas separated by the symbol delimiter. In this case, the signal periods of both symbols can be accurately estimated.

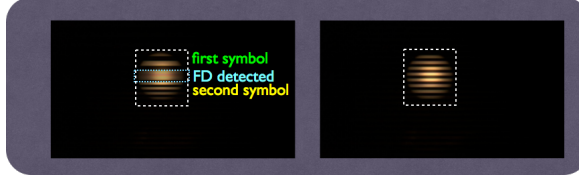


Figure 13: An example flow of the symbol delimiter detection of the receiver end.

The estimated signal period will be mapped to a meta symbol. The meta symbol is then split into a sequence number and a data symbol.

Dropped symbol detection and recovery. Then, the sequence number is used to identify any missing symbol or redundant symbol. Missing symbols will be reconstructed with corresponding parity symbols, while redundant symbols with the same sequence number will be dropped. In the case that redundant symbols with the same sequence number is demodulated to different symbols, the one decoded with the largest image area will be used.

The data string is finally obtained after mapping the sequence of data symbols back to the bit patterns, forming the original bit stream.

4.4 System Components

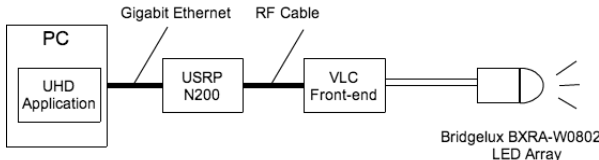


Figure 14: Transmitter Components

As the system is still under development, the developed system should be sufficiently flexible so that it is easy to change various desires of the system, e.g., the modulation format, the protocol design, etc. To this end, we utilize a software-defined radio (SDR) platform in our system, which enables us to make most necessary modifications in software with minimal efforts. Additional hardware components were developed to interface between the SDR and the optical transmitting and receiving components. [Figure 14](#) shows the transmitter components in our proposed VLC system.

In the transmitting end, we use a PC with USRP Hardware Driver (UHD) application to modulate the digital information in a packet into analog signal, in the format of digitized samples. The SDR is connected

to the PC via gigabit Ethernet. The SDR converts the digitized samples sent from the PC into analog signal. The VLC front end board converts the voltage varying signal to current varying signal and outputs that to the LED. The signal would determine the output intensity of the LED.

In the receiving end, we just use a camera to receive the optical signal and use simple computer vision and digital image processing mechanism to demodulate. We use PointGrey Flea3 camera [14], which provides the capability to manually control various camera parameters. We also use a number of smartphones to compare their performance.

In the following, we will describe the components in the system in detail.

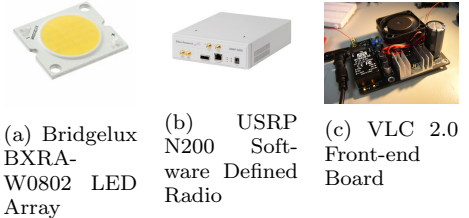


Figure 15: Photos of Transmitter Components



Figure 16: Photos of Receiver Components

4.4.1 LED Array

[Figure 15\(a\)](#) shows the Bridgelux BXRA-W0802 [15], which is a high brightness LED array suitable for indoor illumination purposes and chosen as the transmitting LED component. The maximum DC forward current is 2 amps, and the typical forward voltage is around 13 volts, resulting in a maximum output power of 26 W. Typical luminous flux with 1050 mA forward is 850 lumen.

4.4.2 Software Defined Radio

As a highly flexible tool to realize the traditional RF communications, SDR has become our preferred platform to develop the VLC system. In our system, we

use Ettus Universal Software Radio Peripheral (USRP) N200, as [Figure 15\(b\)](#) shows. USRP then converts the digital signal samples to analog voltage-varying signal. The unit features a gigabit ethernet interface to transfer signal samples to the PC. N200 provides high-bandwidth and high-dynamic range processing capability. A modular design allows the N200 to operate from DC to 6 GHz.

In our system we use a daughter board (LFTX) that is capable of transmitting signals from DC to 30 MHz. N200 can stream up to 50 MegaSample/s to and from host applications, and users can implement custom functions in the FPGA fabric, or in the on-board 32-bit RISC softcore. The FPGA offers the potential to process up to 100 MHz of RF bandwidth in both the transmit and receive directions. This is more than sufficient for our application as VLC usually operates in the range of 0.1 kHz to several kHz. The sampling rate to convert the digital samples to analog signal is configured at 1 MHz. This could emulate the clock rate of a low-cost microcontroller. Inaccuracy in the transmitted signal period could be caused by low sampling rate.

4.4.3 UHD

UHD is a driver developed by Ettus Research and is compatible with all USRP software-defined radios. UHD allows development on multiple operating systems. UHD provides an application programming interface (API), which provides access to various functions of the USRP including synchronization, sample streaming, and configuration.

In the thesis, we modify one of the example applications provided with the UHD software package to modulate the transmitting signals.

4.4.4 VLC Front-end Board

The output light intensity of the LED depends on the magnitude of the input current. Thus, a hardware component is required to interface between the SDR and the LED component, linearly converting a voltage-varying signal to a current-varying signal. We utilize a custom-made VLC front-end circuit board, as shown in [Figure 15\(c\)](#).

One of the main objectives for the design of the front-end board is to accurately convert the level of voltage in the input signal to the level of the output intensity of the attached LED. For example, when the voltage of input signal is zero, the front-end would control the light intensity of the LED to be zero, and when the voltage of the input signal is raised to the maximum, the light intensity of the LED should also at its maximum.

Moreover, this conversion also needs to be done fast enough so that a high frequency signal can be transmitted.

4.4.5 Rolling Shutter Camera

There are a number of cameras used in our experiments. [Figure 16\(a\)](#) shows the specification of Point-Grey Flea3 (FL3-U3-88S2C-C) [14], a high-speed camera built for experimental purposes, thus various parameters such as exposure time can be adjusted to a wide range of values. This allows us to examine system performance in different conditions. [Table 2](#) lists the specification of Point Grey Flea3 camera.

The cameras on smartphones, such as HTC New One and iPhone 5S shown in [Figure 16\(b\)](#), are also selected for some experiments, in order to determine the expected performance of RS-FSK on cameras in off-the-shelf smartphones.

Table 2: Specification of Point Grey Flea3 (FL3-U3-88S2C-C).

Parameter	Value
Camera Sensor Format	1/2.5"
Type of Sensor	Sony IMX121 CMOS
Pixel (H x V)	4096 x 2160, 2048 x 1080
Pixel Size (H x V)	1.55 μ m x 1.55 μ m
Max Frame Rate (fps)	21.6, 60
Type of Shutter	Rolling Shutter
Exposure Time	0.015 ms - 1 s
Estimated Read-out Time	0.01473 ms

5. IMPLEMENTATION

5.1 Encoder

For the transmitting end of the system, we implement a UHD application to generate the signal. It takes a given bit stream, and produces encoded frames following a predefined bit-to-symbol mapping and the frame layout described in the previous subsection. We use 1 MHz sampling rate and a given transmitting frame rate to generate samples within one frame. These samples are then encoded with bit 1s and 0s with the corresponding symbol frequency. The frames are then turned into analog signal and transmitted via LED light.

5.2 Decoder

The decoder is implemented in several programming languages. Two are implemented in Matlab and C++ with OpenCV for post processing and analyzing. The other is implemented in Objective-C with OpenCV as an iOS application for real-time processing. We will evaluate the processing time in [subsection 6.6](#).

6. EVALUATION

In [subsubsection 4.2.2](#), we derive the probability of symbol loss and mixed frame. The value is affected by the transmitting frame rate ($T_{f,tx}$), receiving frame rate

$(T_{f,rx})$, the read-out time of the camera (T_r) and the height of the LED in the received image (H). Therefore, in this chapter we present the experimental results of our unsynchronized VLC system with respect to these factors. The performance metrics we use in the experiments are Packet Reception Rate (PRR) and throughput.

Each symbol represents 4-bit, and thus we have 16 symbols. The symbol-to-frequency mapping table is shown in Table 3.

Here, we will revisit the derivation of P_{miss} previously mentioned in subsubsection 4.2.2. The previous equation only considered the case of a complete symbol loss. However, in reality, we should also consider if part of the symbol is outside the gray area in Figure 8. and if the outside part of the symbol is shorter than $H_{min}T_r$. In this case, the symbol cannot be demodulated and should be considered missing. That is, the outside part of the symbol is not sufficient large to be decoded. Here we assume H_{min} be three times of the widest pixel width we use to transmit, which means we at least can see three black-white strips in the received image. We also deduct the time duration of the symbol delimiter transmission when that symbol is transmitted. Thus, the probability is given by

$$P'_{miss} = \frac{T_{f,rx} - (H - H_{SD})T_r + 2H_{min}T_r - T_{f,tx}}{T_{f,rx}} . \quad (11)$$

6.1 Performance under Different Receiving Frame Rate

First, we want to show the improvement of the decoding performance due to the design of the symbol delimiter, the sequence number, and the parity symbol. We use a Bridgelux LED Array as the transmitter and the PointGrey Flea3 camera configured with 30 fps, as the receiver. Figure 17 shows a photo illustrating our setup.

We alter the receiving frame rate to obtain different tx/rx frame rate ratios from 0.9 to 2 to force unsynchronized transmitter and receiver pairs. That is, we fix the transmitting frame rate at 30 fps, and alter the receiving frame rate from 15 fps to 33 fps. We randomly generate 20 string sequences for each of the three settings: (1) no additional schemes; (2) with only symbol delimiter; and (3) with symbol delimiter, sequence number, and parity symbol. The length of the string sequence is 20 bytes. Note that we also record the videos at random starting time to introduce random phase difference between the transmitter and the receiver.

Figure 18 shows the result. When the receiving frame rate and the transmitting frame rate are very close to each other, the first setting has slightly lower PRR, as a number of received image frame will be mixed with two symbols and a portion of them will be demodulated cor-



Figure 17: Experimental setup photo.

rectly. The other two settings perform similarly. However, as the difference between the frame rates increase, the differences in PRRs become very obvious.

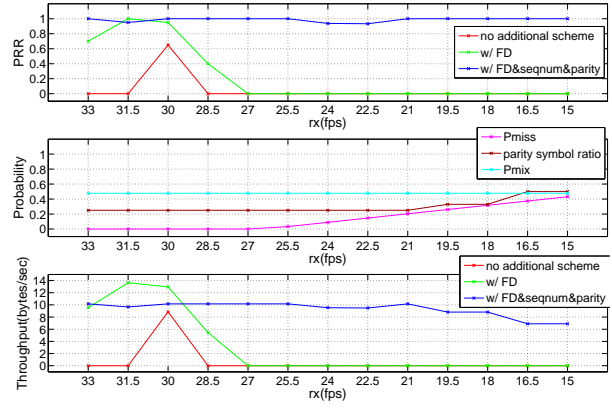


Figure 18: Result under different rx fps.

The P'_{miss} and parity symbol ratio are also shown in Figure 18. For the third setting, we use P_{miss} to determine the number of parity symbols required to be inserted into a packet. When the receiving frame rate is higher than 19.5 fps, the parity symbol ratio is configured to be 0.25, which means for every three symbols, we add a parity symbol. (It is possible to use a parity symbol rate less than 0.25, following the pink line in the figure. However, we do not discuss such a case here, and will discuss the maximum throughput in subsection 6.4.) When the receiving frame rate is between 19.5 and 18 fps, we use a parity symbol ratio of 0.33. When the receiving frame rate is lower than 18 fps, we use a parity symbol ratio of 0.5, which means for every symbol, we transmit twice. With all 3 schemes, close to 100% of the packets are received correctly, while the other two settings rapidly lose the ability to receive correct packets when the difference between frame rates increases. The results verify that our design can indeed address the issues caused by unsynchronized transmitter and receiver pair.

We can see when the receiving frame rate and the transmission frame rate are close, the setting with the symbol delimiter has the highest throughput. As the difference between the frame rates increases, the through-

Table 3: symbol-to-frequency mapping table

symbol	seq_num 0 frequency / pixel width	seq_num 1 frequency / pixel width	seq_num 2 frequency / pixel width
preamble	5657.3886 / 6	x	x
symbol delimiter	4849.1902 / 7	x	x
EOF	3771.5924 / 9	x	x
0000	3394.4331 / 10	1305.5512 / 26	808.1984 / 42
0001	3085.8483 / 11	1257.1974 / 27	789.4031 / 43
0010	2828.6943 / 12	1212.2975 / 28	771.4620 / 44
0011	2611.1024 / 13	1170.4941 / 29	754.3185 / 45
0100	2424.5951 / 14	1131.4777 / 30	737.9202 / 46
0101	2262.9554 / 15	1094.9784 / 31	722.2198 / 47
0110	2121.5207 / 16	1060.7603 / 32	707.1736 / 48
0111	1996.7254 / 17	1028.6161 / 33	692.7415 / 49
1000	1885.7962 / 18	998.3627 / 34	678.8867 / 50
1001	1786.5438 / 19	969.8380 / 35	665.5751 / 51
1010	1697.2165 / 20	942.8981 / 36	652.7756 / 52
1011	1616.3967 / 21	917.4144 / 37	640.4590 / 53
1100	1542.9241 / 22	893.2719 / 38	628.5987 / 54
1101	1475.8405 / 23	870.3674 / 39	617.1697 / 55
1110	1414.3471 / 24	848.6082 / 40	606.1487 / 56
1111	1357.7733 / 25	827.9105 / 41	595.5146 / 57

put of the third setting decreases due to the large parity symbol ratio.

6.2 Performance under Varying Inter-frame Interval

According to [3], the receiving frame rate of smartphone cameras exhibit more variability for several reasons. Even when the average frame rate appears steady, the inter-frame interval still varies. In order to show the improvement with our new design scheme, we emulate this phenomena with a system with time varying inter-frame interval. However, it is hard to alter the receiving frame rate while receiving frames. We therefore use the Flea3 camera with fixed receiving frame rate and alter the transmitting frame rate before transmitting every symbol. To simulate the various of transmitting frame rate, we use a truncated normal distribution with the mean value of 36.9458 fps, the standard deviation of 3.94, the min value 31.03 fps and the max value 42.86 fps. The normal distribution of various transmitting frame rate is shown in Figure 19. The values are based on observations presented in [3], which states that the receiving frame rate fluctuates significantly between 21 to 29 fps for an entirely white foreground, with an average of around 25 fps. Figure 20 shows the generated random numbers for each transmitting frame.

We again generate 20 random string sequences. The length of each string sequence is 20 bytes. For each transmitting symbol, we randomly pick a number from the truncated normal distribution and transmit the sym-

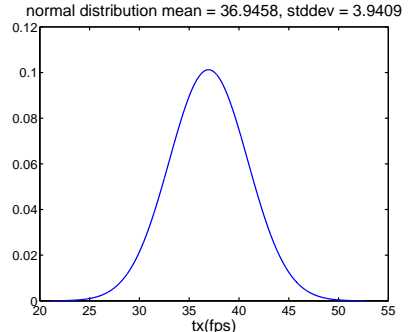


Figure 19: Normal distribution of various transmitting frame rate.

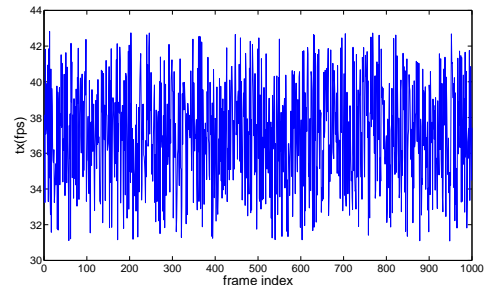


Figure 20: Generated random numbers from the normal distribution in Figure 19.

bol with the generated frame rate. We use the Point-Grey Flea3 camera to record the video at fixed 30 fps.

Table 4 shows the result of PRR and throughput. First, we want to know how frequently mixed frame or lost symbol occur. Thus, we use the average transmitting frame rate 36.9458 fps to calculate the probability. We get $P_{miss} = 0.0501$ and $P_{mix} = 0.5877$. We can see that with no additional schemes, the PRR is 0 since there are a large number of mixed frames. With only the symbol delimiter setting, the PRR is still 0 because there is a non-zero probability to have missed symbol. With all three schemes, the PRR is 1. It is worth mentioning that we use a lower parity symbol ratio to increase the throughput in this experiment.

Table 4: PRR and Throughput under various inter-frame interval.

Setting
No additional schemes
With only symbol delimiter
With symbol delimiter, sequence number and parity symbol
With symbol delimiter, sequence number and parity symbol
With symbol delimiter, sequence number and parity symbol
With symbol delimiter, sequence number and parity symbol

6.3 Performance under Different Smartphone Cameras

Third, we use several smartphones to compare the coding performance under the three previous mentioned settings. **Table 5** lists the phones and their specifications.

Table 5: Summary of camera parameters of different smartphone devices.

Device and Camera	Image Resolution ($X_{max} \times Y_{max}$)	Frame Duration (ms)
Point Grey Flea3	2048x1080	30
Apple iPhone 5s Back	1920x1080	29.98
Apple iPhone 5s Front	1280x720	29.98
HTC New One Back	1920x1080	29.94
HTC New One Front	1920x1080	29.6
Samsung Galaxy S4 Back	1920x1080	29.93
Samsung Galaxy S4 Front	1920x1080	29.91

Note that the receiving frame rate of the smartphones are not fixed. Moreover, the read-out time and the resolution of the camera of smartphones are also different. These will affect the probabilities of symbol loss and mixed frame. We again generate 20 random string sequences. The length of each string sequence is 20 bytes. **Figure 21** shows a photo illustrating the experimental setup. In this experiment, we place a lampshade on the top of the LED to diffuse the light.



Figure 21: Experimental setup photo.

According to **Table 5**, the read-out time of the smartphones are not the same. This means different smartphone cameras observe different pixel width (signal period) under the same transmitting frequency. Therefore we use the preamble symbol to calibrate the throughput of the different pixel widths of all the different pixel widths of different smartphone cameras. **Figure 22** shows the pixel width of different smartphone cameras. We use the pixel width of Flea3 as the base (the X-axis), and the Y-axis represents the observed pixel width. Generally, the pixel width grows linearly. What we need to do is to calibrate the lines to fit the top black line.

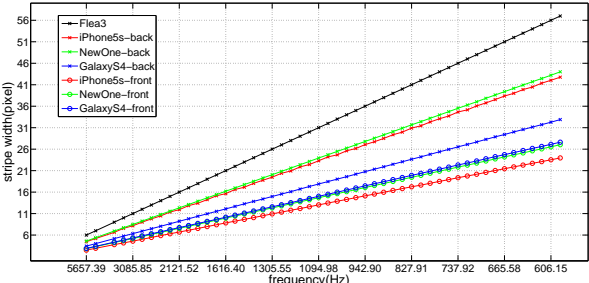


Figure 22: Pixel width under different smartphone devices.
Frame Duration (ms) | Frame Duration (ms)
14.73 | 17.42 (52.26%)
19.64 | 12.15 (36.42%)

First, we use the preamble symbol for the calibration. After determining the pixel width of the preamble symbol, we calculate the ratio between the expected pixel width of our base calculated with the images captured by Flea3 camera (which is around 6 pixel) and the pixel width calculated with the images captured by the smartphone camera. Then, for each received pixel width, we multiply the ratio and calculate the error. **Figure 23** shows the absolute difference between the expected pixel width of Flea3 and the calibrated pixel width of smartphone devices. We can see as the pixel width grows, the error gets larger which can be as large as 1 pixel. If the error is larger than 0.5 pixel, it could be determined as a neighboring symbol and it would result in an erroneous symbol. The reason why the cal-

ibrated pixel width do not work well is that the camera sensor on the smartphones produce more noise in the image compared to the one of the Flea3. As a result, if the pixel width is too small (say, less than 15 pixel), it will have a higher error probability. The result implies that the pixel width of current preamble symbol is too small.

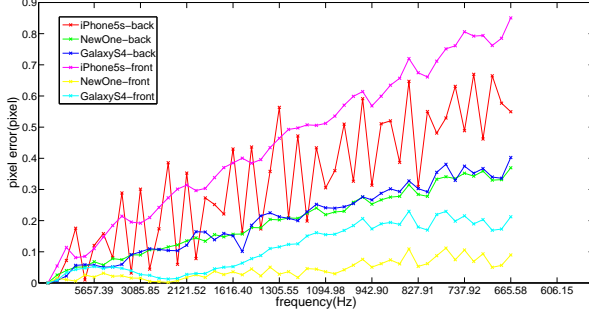


Figure 23: Pixel error when using the symbol with the smallest signal period as the preamble.

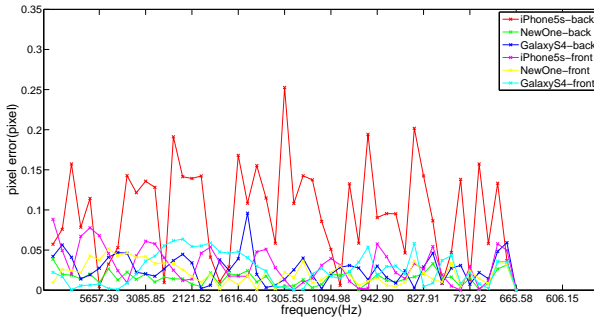


Figure 24: Pixel error when using the symbol with the largest signal period as the preamble.

To address this issue, we instead use the one with the largest pixel width as the preamble symbol. For the third setting, we use the frequency merely lower than the last transmitting symbol in Table 3, which is 585.24 Hz. With this symbol, the expected pixel width of Flea3 is around 58 pixel. We again calculate the ratio and the calibrated pixel width. Figure 24 shows the result of error. We can see that the pixel error of most devices is now smaller than 0.1 pixel. However, the back facing camera of the iPhone5s still has larger error, though also lower than 0.25 pixel, which is acceptable. For the first and second settings, we use the frequency lower than the last transmitting symbol, which is 1305.5512 Hz. With this symbol, the expected pixel width of Flea3 is around 26 pixel.

Figure 25 shows the result. The X-axis shows different smartphone cameras. We first calculate P_{miss} by averaging the frame rate of each smartphone camera.

The obtained values are all zeros since the average fps are close to 30. However, we can see that P_{mix} is high.

For the first setting, we can see the PRR is about 50% to 60%. The result also shows that when the P_{mix} is higher, PRR of the first setting gets lower. For the second and third settings, basically that PRRs are similar since no symbol miss take place. However, we can see that most of the devices show that the third setting gets lower PRR than the second setting. Some of the devices also show that the third setting gets lower PRR than the first setting. Furthermore, the overall PRR is on the low side. We think the problem is due to decoding error. Because of the instability of the smartphone cameras, if the received pixel width of the preamble has slightly error, it will affect the third setting very much because the pixel width range we use in the third setting is larger than the first two settings. The yellow and cyan bars in the figure represent the result ignoring the preamble error. We can see that PRRs of the second and third settings are very close to 1. (From this experiment, we can see that the second setting is good enough for the communications in spite of using different smartphones. However, the current setting uses regular video recording mode rather than preview mode, and the receiver is very close to the transmitter. That is, there are many factors not considered yet and these will be discussed in the following subsection.) Therefore, the error are mainly caused by the preamble calibration rather than the unsynchronized issues. To address the preamble calibration error, we can transmit more preamble symbols at the beginning of the packet and average them when receiving these symbols. This solution can minimize the error caused by calibration but will increase the packet overhead at the same time.

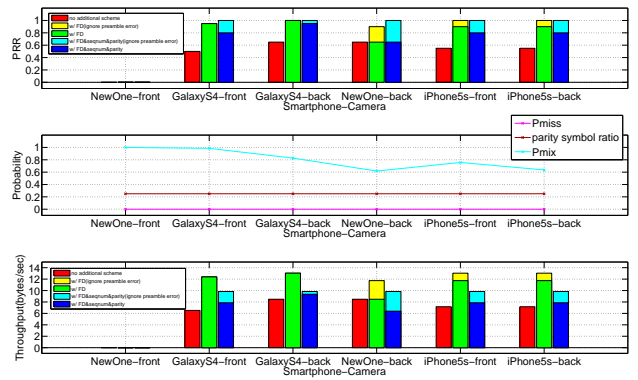


Figure 25: Result under different smartphone devices.

We also found that the front-facing camera of HTC NewOne cannot decode any packet in all three settings. We observed that the behavior of the camera records every frame twice. Even when we extract half of the frames in the video, it is still not able to decode. Therefore, we think the problem is not related to our decoding

method. Our results indicate that, the second setting can obtain the maximum throughput in most settings.

6.4 Max Throughput under Different Transmitting Frame Rate

In this experiment, we fix the receiving frame rate and gradually increase the transmitting frame rate to determine the maximum achievable throughput, and when we can achieve it. As the transmitting frame rate gets higher, P_{miss} increases, and thus we need to use a higher parity symbol ratio to compensate. However, the transmitted data rate also increases. We would like to investigate at what transmitting frame rate the maximum throughput can be obtained. In this experiment, we increase the transmitting frame rate from 33 fps to 90 fps. Two cameras are used in this experiment. The receiving frame rate of Flea3 is fixed at 30 fps. The iPhone5s is at 29.98 fps on average. We only use the third setting in this experiment.

[Figure 26](#) shows the results of Flea3. We can see P_{miss} grows from 0 to over 0.5, and the parity symbol ratio we select is just above the P_{miss} line. Note that the parity symbol ratio we use is at most 0.5. Because we think the overhead costs too much if a symbol is transmitted over two times. We can see that PRR is more than 90% until the transmitting frame rate reaches 81 fps. Theoretically, the upper limit of the transmitting frame rate is bounded by the case of having two symbols in a received frame, which is given by

$$FPS_{Max,tx} = \frac{1}{(H - 2H_{SD})T_r} . \quad (12)$$

The max transmitting frame rate for iPhone5s is about 53.39 fps, and 74.44 fps for the Flea3. However, two symbols in a received frame rarely happens. At that time the parity symbol can be used to recover data. Therefore, we can get even higher transmitting frame rate in practice.

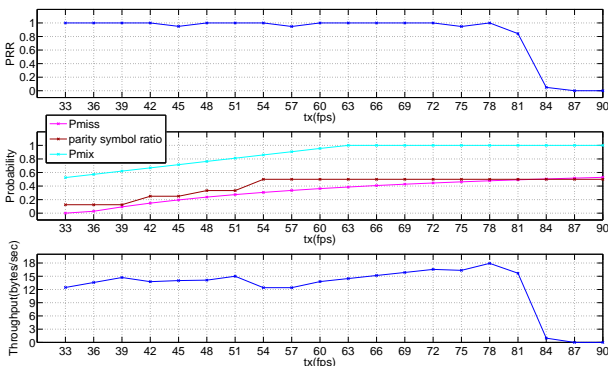


Figure 26: Result of Flea3 under different transmitting frame rate.

[Figure 27](#) shows the result of iPhone5s. Compared to Flea3, P_{mix} grows faster while P_{miss} grows slower.

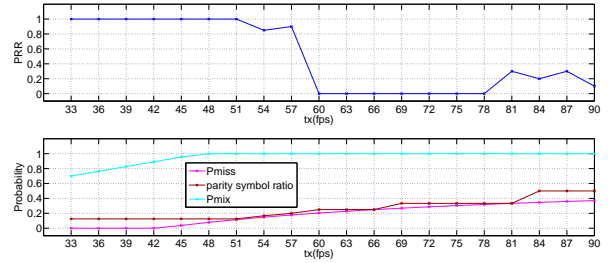


Figure 27: Result of iPhone5s under different transmitting frame rate.

We can see that PRR reaches 0 at 60 fps. We analyzed the data and found that P_{miss} meets our expectation at this transmitting frame rate but the distribution of the missing symbols is uneven. The two missing symbols can be found in three consecutive frames, which means the parity symbol ratio is not sufficient. To address the issue, we increase the parity symbol ratio to 0.5 after 60 fps and [Figure 28](#) shows the modified result. The PRR is above 80% until reaches the transmitting frame rate of 81 fps. We can see that both Flea3 and iPhone5s can have high PRR when the transmitting frame rate is lower than 81 fps.

We can see the throughput line grows with a trend - at the time the parity symbol ratio increases, the throughput would stay the same or drop a little. The maximum throughput of Flea3 happens at 78 fps, and the throughput has increased by 1.2 times and reaches 18 bytes per second. The maximum throughput of iPhone5s happens at 51 fps, and the throughput has increased by 1.28 times and reaches 19.25 bytes per second.

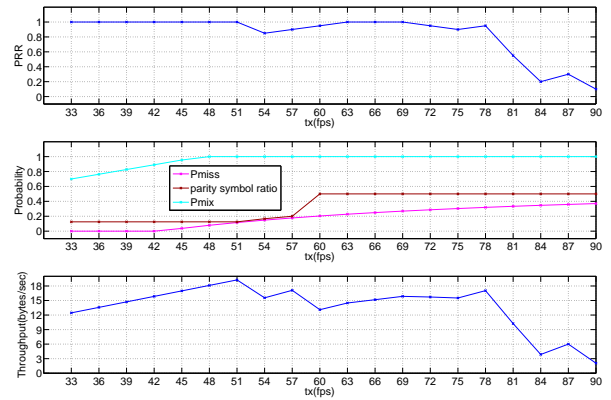


Figure 28: Modified Result of iPhone5s under different transmitting frame rate.

6.5 Performance under Different LED Size in the Image

So far, we have considered the factors of transmitting frame rate, receiving frame rate and the read-out time of the camera. There is one more factor - the image

height, which may affect P_{miss} and P_{mix} . Thus, in this experiment, we try to change the height of the LED in the received image. There are two methods to do so, one is use the same setting with the previous experiments (which let the LED light full of the image) and simply crop the image into the height we want. The other is to move the receiver from near to far. We choose the latter method. When we get far away from the LED, although the intensity of light and the detection of the LED boundary may also cause some decoding error, we think the latter method exhibits a setting closer to the real situation.

We use the height (pixel) of the LED in the received image as our X-axis in [Figure 30](#). The transmitting frame rate is configured to 30 fps. We use two cameras in this experiment. The Flea3 has a fixed receiving frame rate at 30 fps. The iPhone5s is at 29.98 fps on average. We only use the third setting in this experiment. As to how far away we can reach, it depends on the sensor size of the camera, the focal length of the lens, and the size of the LED. [Table 6](#) lists the parameters of the cameras we use in the experiment. If we know all the above parameters, the distance from the LED to the camera is proportional to:

$$distance(cm) \propto \frac{focal_length(mm) * LED_height(mm) * image_height(pixel)}{LED_height(pixel) * sensor_height(mm)} \quad (13)$$

We also provide a comparison in [Table 7](#), showing the relationship between the distance and LED height in the received image of Flea3 and iPhone5s. The real LED height we use in the experiment is 4.7 cm. In the table, we can see if the LED object in the image is around 500 pixel, the distance from the object to the Flea3 can be half a meter, while the iPhone5s can only be 15 centimeters. However, if the size of the image area illuminated by the light becomes bigger, (For transmitter-end, we can simply use the lampshade to enlarge the light range. For receiver-end, we can use the reflected light from surrounding areas, such as a wall.) we can further lift the distance limitation.

[Table 6](#): Camera parameters of Flea3 and iPhone5s.

Parameters	Flea3	iPhone5s
Camera Sensor Format	1/2.5"	1/3"
Image Height(pixel)	1080	1080
Pixel Size(μm)	1.55	1.5
Focal Length(mm)	16	4.21

[Figure 29](#) shows a photo illustrating the experimental setup. Note that we still have a limitation that the transmitting symbol in the received image need to occupy at least two black-white strips for detecting the signal period. For example, symbol with the largest

strip width received from Flea3 is 58 pixel, so the image area need to have at least a height of 232 pixel. It means if the height of LED in the received image is smaller than 232 pixel, then the received symbol cannot be decoded.

[Table 7](#): Distance table of Flea3 and iPhone5s.

LED height in image (pixel)	1000	900	800	700	600	500
Flea3 distance (cm)	48.5	53.9	60.6	69.3	80.9	97.1
iPhone5s distance (cm)	7.75	8.61	9.68	11.07	12.91	15.4

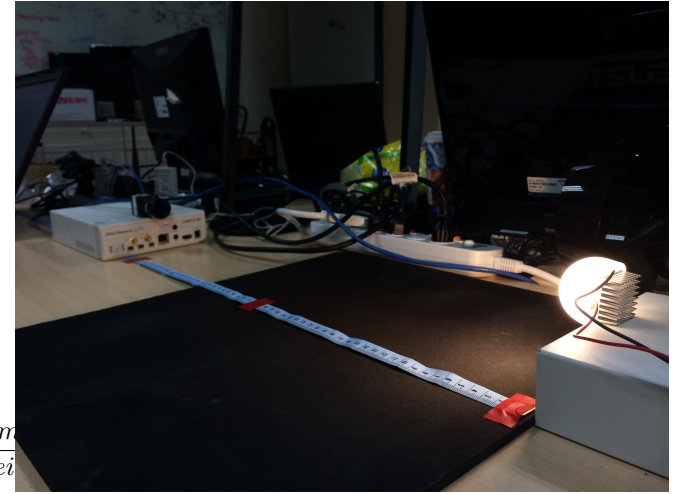


[Figure 29](#): Experimental setup photo.

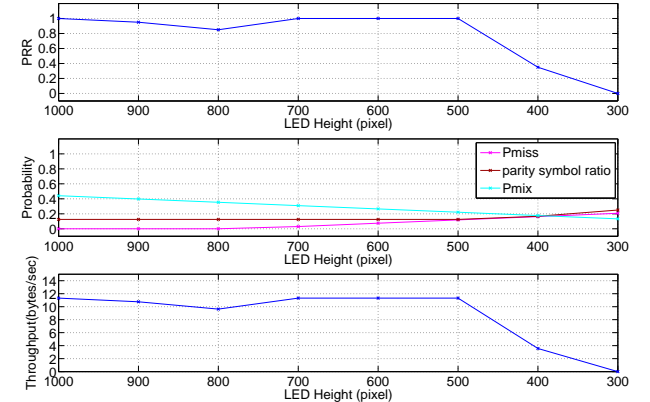


[Figure 30](#): Result of Flea3 under different LED height.

[Figure 30](#) shows the results of Flea3. As the LED object in the image becomes small, P_{mix} slightly goes down, and P_{miss} slightly goes up. Note that P_{miss} here is not caused by the whole missing symbol in the received image. It means that the transmitting symbol in the received image is too short to be decoded. This happens when the symbol delimiter appears in the received image and the upper part and lower part of the symbol in the image do not have enough pixel width. We

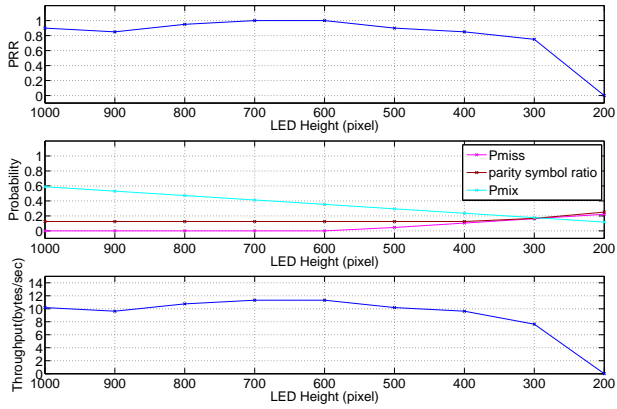


Figure 31: Result of iPhone5s under different LED height.

can see when the LED height is around 400 pixel, the PRR starts to drop. When the LED height is below 400 pixel, it cannot be decoded at all. Although P_{mix} is not very high, the symbol delimiter can always appear in the consecutive frames together since the transmitting frame rate and the receive frame rate are close, consecutive symbol losses are observed. Therefore, it does not work even if we use a higher parity symbol ratio.

iPhone5s, as shown in Figure 31, due to its longer read-out time and shorter time gap between receiving frames, P_{miss} is relatively smaller. Thus, when the LED has a height of around 300 pixel in the image, the transmission can still be received. The PRR is about 75%.

We can see both Flea3 and iPhone5s can achieve $9.5 \sim 12$ bytes per second when the LED height is above 500 pixel. As the LED object in the image becomes small, the throughput decreases significantly; due to both a smaller PRR and a large parity symbol ratio.

6.6 Time Measurement of Real-time iOS Decoder App

We have shown that our system work well for cameras on mobile devices. In this subsection, we want to know whether the decoding process can be executed in real-time with smartphone processors, we also implement an iOS decoding app, running on iPhone5s.

We use the AV Foundation framework, which provides an Objective-C interface for managing and playing audio-visual media in iOS applications. The application uses multiple threads. One thread obtains the frame buffers captured by the camera, and put the image buffers into the queue to be processed. The other thread takes the frame at the front of the queue and decodes it in real time without saving the image. Decoding results for the frame will be shown on the phone screen. Figure 32 shows the GUI of the iOS application; one can first touch the screen where the light locates to lock the focus and the exposure time. After pressing

start button, the application will start to detect the LED location and decode the message.

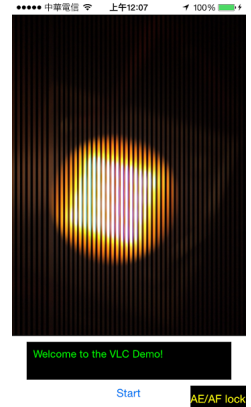


Figure 32: iOS application GUI

Since we have set the FrameDuration of the captured video data output (for example, we set the video to 30 fps), we need to make sure that we have enough time to process a frame within one FrameDuration.

To optimize the processing time, we first add the optimization level of Apple LLVM 5.1 compiler as "-Os", generating a faster and smaller executable.

Next, we time individual operations to assess their computational complexity. We found that the majority of the processing time happens when we try to get the frame buffer and convert it to the UIImage, then convert the UIImage to the OpenCV Mat type. This step takes about 0.04 sec, which is greater than a frame duration. To reduce the time, we directly get the pixel base address and put it into Mat. Surprisingly, the time reduces to 0.00003 sec.

Moreover, we found that when we convert RGB to gray scale, it also costs about 0.02 sec. To reduce the time, we change the video output pixel format to YUV color space, and use the luminance(Y) channel as the gray scale value. As a result, we save 0.02 sec.

After a series of optimizing steps, the total processing time of a frame is about 0.007 sec which is less than 1/30 sec. Since our current implementation already meets the real-time target, we do not explore further optimizations, even though some operations could be sped up more. Table 8 lists the time taken for each operation.

7. CONCLUSION AND FUTURE WORK

7.1 Conclusion

In this thesis, we implemented a CamCom system that utilizes a **single LED** as the transmitter and a common **rolling shutter CMOS camera** as the receiver. We presented considerations for addressing issues caused by unsynchronized transmitter and receiver,

Table 8: Processing time breakdown in ms

Operation	time(ms)
Image Buffer to Mat Conversion	0.03
Symbol Delimiter Detection	3.25
YIN Period Detection	3.74
GUI Text Output	0.04
Total	7.06

including the introduction of **symbol delimiter**, **sequence number**, and **parity symbol** in the transmission. In each situation, we calculate the probability of symbol loss and mixed frame first, then decide which setting is suitable and adjust the parity symbol ratio by the probability.

Experimental results confirm that the additional designs would significantly improve the packet reception rate (PRR) from 0.6 to 0.99 when the transmitting and receiving frame rates are close. We also can improve the PRR from 0.0 to 0.8~1.0 even when the transmitting and receiving frame rates have a large difference or when the the receiving frames have varying inter-frame intervals. A variety of front/ back-facing cameras of smartphones can be used in our system without any modification. One can increase the throughput by 1.2 times by increasing the transmitting frame rate. Data still can be received when the height of LED object in the image is more than 400 pixel. The overall throughput reaches 18 bytes per second. The decoding application proves that series of step can be processed in real-time, with each image frame completely demodulation in merely 7 milliseconds.

7.2 Future Work

Improve the iOS real-time decoding app. There are many things can be improved. First is the LED detection. For now, we just threshold the image to binary and find the bright part as the boundary. However, it is not an efficient way and is affected by the surrounding light noise. We want to adopt the characteristics of the strips and use some Digital Image Processing (DIP) techniques to figure out. On the other hand, to get shorter exposure time, the current method is to move the camera to be very close to the LED light and lock the exposure time. It is not convenient in the real life scenarios since we are not able to get very close to the light. The Landmark paper [10] have proposed the algorithm which find the brightest part in the image then focus/ expose at it, which could be adapted to our system.

Increase the data rate. There are severals ways to increase the data rate, we have tried increasing the transmitting frame rate. We also can increase the number of bits represented by each symbol. We can obtain a higher data rate with more transmitting symbols to

carry the bits.

Consider more scenarios. Currently we focus on the static environments. We still need to do more experiments in the moving scenario or dynamic environments to access the feasibility and reliability of our design.

8. ACKNOWLEDGEMENTS

test intro

9. REFERENCES

- [1] S. D. Perli, N. Ahmed, and D. Katabi, “Pixnet: interference-free wireless links using lcd-camera pairs,” in *Proceedings of Mobile computing and networking*. ACM, 2010, pp. 137–148.
- [2] T. Hao, R. Zhou, and G. Xing, “COBRA: color barcode streaming for smartphone systems,” in *Proceedings of Mobile systems, applications, and services*. ACM, 2012, pp. 85–98.
- [3] W. Hu, H. Gu, and Q. Pu, “LightSync: unsynchronized visual communication over screen-camera links,” in *Proceedings of Mobile computing and networking*. ACM, 2013, pp. 15–26.
- [4] G. Woo, A. Lippman, and R. Raskar, “Vrcodes: Unobtrusive and active visual codes for interaction by exploiting rolling shutter,” in *Proceedings of the 2012 IEEE International Symposium on Mixed and Augmented Reality (ISMAR)*, ser. ISMAR ’12. Washington, DC, USA: IEEE Computer Society, 2012, pp. 59–64. [Online]. Available: <http://dx.doi.org/10.1109/ISMAR.2012.6402539>
- [5] A. Ashok, M. Gruteser, N. Mandayam, J. Silva, M. Varga, and K. Dana, “Challenge: Mobile optical networks through visual mimo,” in *Proceedings of the Sixteenth Annual International Conference on Mobile Computing and Networking*, ser. MobiCom ’10. New York, NY, USA: ACM, 2010, pp. 105–112. [Online]. Available: <http://doi.acm.org/10.1145/1859995.1860008>
- [6] A. Ashok, M. Gruteser, N. Mandayam, T. Kwon, W. Yuan, M. Varga, and K. Dana, “Rate adaptation in visual mimo,” in *Sensor, Mesh and Ad Hoc Communications and Networks (SECON), 2011 8th Annual IEEE Communications Society Conference on*, June 2011, pp. 583–591.
- [7] M. Varga, A. Ashok, M. Gruteser, N. Mandayam, W. Yuan, and K. Dana, “Demo: Visual mimo based led - camera communication applied to automobile safety,” in *Proceedings of the 9th International Conference on Mobile Systems, Applications, and Services*, ser. MobiSys ’11. New York, NY, USA: ACM, 2011, pp. 383–384. [Online]. Available: <http://doi.acm.org/10.1145/1999995.2000046>

- [8] R. D. Roberts, "Undersampled frequency shift ON-OFF keying (UFSOOK) for camera communications (CamCom)," in *Proceedings of Wireless and Optical Communication Conference*. IEEE, May 2013, pp. 645–648.
- [9] C. Danakis, M. Afgani, G. Povey, I. Underwood, and H. Haas, "Using a CMOS camera sensor for visible light communication," in *Proceedings of Globecom Workshops*. IEEE, Dec 2012, pp. 1244–1248.
- [10] N. Rajagopal, P. Lazik, and A. Rowe, "Visual light landmarks for mobile devices," in *Proceedings of the 13th International Symposium on Information Processing in Sensor Networks*, ser. IPSN '14. Piscataway, NJ, USA: IEEE Press, 2014, pp. 249–260. [Online]. Available: <http://dl.acm.org/citation.cfm?id=2602339.2602367>
- [11] J. Nakamura, *Image Sensors and Signal Processing for Digital Still Cameras*. Boca Raton, FL, USA: CRC Press, Inc., 2005.
- [12] A. El Gamal and H. Eltoukhy, "CMOS image sensors," *Circuits and Devices Magazine*, vol. 21, no. 3, pp. 6–20, 2005.
- [13] A. De Cheveigné and H. Kawahara, "Yin, a fundamental frequency estimator for speech and music," *The Journal of the Acoustical Society of America*, vol. 111, no. 4, pp. 1917–1930, 2002.
- [14] "PointGrey Flea3 Product Datasheet," http://www.ptgrey.com/products/flea3/Flea3_Datasheet.pdf.
- [15] I. Bridgelux, "Bridgelux ES array series product data sheet." [Online]. Available: http://media.digikey.com/pdf/Data%20Sheets/Bridgelux%20PDFs/ES_Array_Series.pdf